NANO LETTERS

2007
Vol. 7, No. 12
3633−3638

A Dielectrophoretic Method for High Yield Deposition of Suspended, Individual Carbon Nanotubes with Four-Point Electrode Contact

Timo Schwamb,[†,‡] Tae-Youl Choi,[‡] Niklas Schirmer,[‡] Nicole R. Bieri,[‡] Brian Burg,[‡] Joy Tharian,[§] Urs Sennhauser,[§] and Dimos Poulikakos*[,‡]

Laboratory of Thermodynamics in Emerging Technologies, Department of Mechanical and Process Engineering, ETH Zurich, Zurich, Switzerland, and Electronics/Metrology Laboratory, EMPA, Zurich, Switzerland

Received July 30, 2007; Revised Manuscript Received September 30, 2007

ABSTRACT

We have investigated new methods to manufacture four-point contacted suspended, individual multiwalled carbon nanotubes by dielectrophoresis. The necessity of four-point contacted carbon nanotubes is underpinned by the need for more exact measurements of carbon nanotube properties and more complex carbon nanotube based devices. In the experimental study herein, we first evaluated the most important dielectrophoretic parameters of two-point electrode structures. The knowledge gained from this step was applied to the deposition of suspended, individual multiwalled carbon nanotubes over two different four-point electrode designs, a 2-D chip design and a novel 3-D chip design. Our results show that the novel approach using three dimensions for the chip design is superior to the current state of the art 2-D designs. We report a highly improved deposition yield of carbon nanotubes over 3-D chips, which will facilitate the reliable design and manufacturing of future carbon nanotube-integrated devices.

The discovery of carbon nanotubes (CNTs) has inspired the research of various disciplines. Researchers in a host of disciplines, ranging from physics to material sciences and engineering, are investigating the unique properties of CNTs, a necessary condition to their implementation in nanotechnology devices.

An obstacle to the research and engineering applications of nanometer sized materials, such as CNTs, is their manipulation, which includes the controlled positioning and precise integration of these materials into micro-electro-mechanical systems (MEMS). To date, two methods of manipulating CNTs have attracted significant research interest: (1) the directed CNT growth onto a desired position of a MEMS,[1] (2) the postsynthesis deposition of CNTs via dielectrophoresis (DEP).[2]

DEP is a method in which an electric dipole, e.g., a CNT, is exposed to an inhomogeneous electric field between electrodes. The electric field gradient exerts a net force on the electric dipole by which the electric dipole can be deposited to a designated position. The relation for the dielectrophoretic net force $\mathbf{F}$ is given by $\mathbf{F} = (\mathbf{p}\cdot\nabla)\mathbf{E}$ with the dipole moment $\mathbf{p}$ and the electric field gradient $\nabla\mathbf{E}$.[3−5] For a CNT the geometry can be assumed as a long prolate spheroid so that the induced dipole moment is described by $\mathbf{p} = {}^1/_2\pi r^2 l \epsilon_m \mathrm{Re}(K)\mathbf{E}$, where the radius and the length of the CNT are denoted by r and l, respectively, the absolute permittivity of the solvent by ϵ_m, and the real part of the complex polarization factor by $\mathrm{Re}(K)$.[4]

For relatively simply structured MEMS, in which two opposing electrodes build the interface for the connection between CNT and MEMS, DEP has already proven its potential for the mass fabrication of CNT-integrated microchips.[2] Making use of these simple CNT-electrode structures, researchers have presented applications like field-effect transitors,[6] integration techniques of CNTs into MEMS,[7] and sensors.[8] Nevertheless, more complex CNT-electrode structures are desired to enable new application possibilities for CNTs.

The aim of this Letter is to present a method realizing the deposition of suspended, individual multiwalled CNTs (MWCNTs) with superior yield and accuracy over four-point electrode structures. A first application of four-point contacted suspended, individual MWCNTs is to measure material properties of MWCNTs more exactly. The research interest in four-point contact structures underpins its importance.[9−14] Among the investigated methods for four-

* To whom correspondence should be addressed. E-mail: dimos.poulikakos@ethz.ch.
† E-mail: tschwamb@ethz.ch.
‡ ETH.
§ EMPA.

10.1021/nl071853t CCC: $37.00
Published on Web 11/13/2007

point CNT contacting, one can differentiate between such methods in which CNTs are randomly placed over a substrate and such methods in which CNTs are deposited onto a desired position. For the electrical contacting, randomly placed CNTs require a three-step procedure: In the first step the positions of the CNTs on the substrate are located by an atomic force microscope (AFM) or scanning electron microscope (SEM). In the second step the located positions are marked and in the third step the CNTs are contacted with the electrodes. The time intensive search is a major drawback. Additionally, such a method does not allow suspended CNTs deposition. Dohn et al.[9] used movable microcantilevers, which served as contacting electrodes. Instead of movable electrodes Ebbesen et al.[12] and Schoenenberger et al.[13] formed metal electrodes on top of CNTs by focused-ion beam and evaporation, respectively.

Different methods for the deposition of CNTs directly to a desired position have been discussed in the literature. Lewenstein et al.[10] deposited CNTs over four premanufactured electrodes using amino-functionalized regions to which CNTs adsorb preferentially. Instead of the surface of the desired deposition position, Klinke et al.[11] functionalized the CNTs themselves. The functionalized CNTs were adsorbed by designated surfaces and electrodes were built over the adsorbed CNT subsequently. Gao et al.[14] placed an individual CNT between two opposing metal electrodes and realized a four-point contacting. To achieve this goal, they placed two additional CNTs acting as electrodes on top of the first CNT by using an AFM.

The focus of this work was to devise a method enabling high deposition yield of suspended, individual MWCNTs over four-point electrode structures. Our aim was to avoid time-consuming pretreatment processes for CNTs and other processes that hinder a mass production of CNT devices, e.g., AFM manipulation. In this Letter we present such a method, which overcomes drawbacks of earlier approaches. Furthermore, we studied DEP parameters and their effect on the deposition yield with a set of two-electrode chips, so-called "test chips", whose results were subsequently utilized in the investigation of the deposition of MWCNTs over four-point electrode chips.

For the deposition of individual MWCNTs over four-point electrode chips we developed two different chip designs, named 2-D design and 3-D design.

The 2-D chips were designed such that four separated platinum (Pt) electrodes generate an electric field that guides the CNT to the desired position. These structures were manufactured by light lithography followed by focused-ion beam (FIB) treatment in a FIB source (FEI Strata 400). Wafers of 100-silicon with a coating of 500 nm silicon nitride (SiN) served as the basis for the light lithography. On top of the SiN layer 100 nm thick Pt structures have been built by light lithography, physical vapor deposition, and subsequent lift-off. The Pt structures consisted of a rectangular Pt electrode at the center of each chip, connected to four separated bonding pads by Pt lines (Figure 1(I)). In a first step of posttreatment four electrodes have been structured out of the center rectangle by FIB milling with a current of

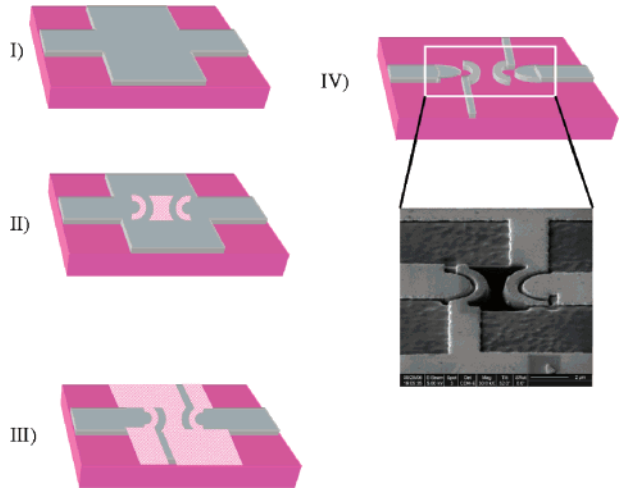

Figure 1. Manufacturing process of 2-D chips: (I) Pt structures built by lift off on SiN wafer; (II) define electrodes by cutting out hatched areas by FIB milling; (III) electrically separate electrodes from each other; (IV) final 2-D design and SEM picture of a 2-D chip.

300 pA of gallium ions (Ga). This first milling step included the cutting out of a sand clock shape in the center of the Pt rectangle and two half-annular shapes each with a spacing of 200 nm to the right- and left-hand side of the sand clock shape (Figure 1(II)). In a second milling step the Pt connection lines between each electrode and its bonding pad were separated from each other (Figure 1(III)). Thus we realized two elliptic shaped outer electrodes and two round shaped inner electrodes electrically separated from each other (Figure 1(IV)). Figure 1(IV) shows a SEM picture of the final design.

Because the deposition of individual CNTs onto conventional chips often results in small deposition yields, which will be discussed later, we designed and manufactured a novel 3-D chip. This is also based on SiN coated 100-silicon wafers. The innovative 3-D chip consists of a three-layer structure of two Pt layers isolated by a SiN layer on top of the basic SiN layer. The Pt structures of both Pt layers were built by the standard techniques of light lithography, physical vapor deposition, and subsequent lift-off. The Pt structures within the first Pt layer are 100 nm thick (Figure 2(I)). After the first lift-off, the entire wafer was coated in a plasma-enhanced chemical vapor deposition process (PECVD) with an 80 nm thick layer of SiN (Oxford Instruments PECVD 80+ machine) (Figure 2(II)). Finally, a second layer of Pt structures was built on top of the SiN layer by light lithography, physical vapor deposition, and lift-off. Figure 2(III) shows the Pt structures on the 3D-chip after the final lift-off. The structures of the two different Pt layers can be distinguished by their color, which is due to the SiN layer in between. The area where the two Pt structures overlap forms the basis for electrodes. This area is located at the center of the Pt structures.

The chip processing was finished by separating the Pt structures in each layer to form electrodes and a gap in between. Here, we again utilized the FIB source and its ability to mill materials at the nanometer scale. The desired

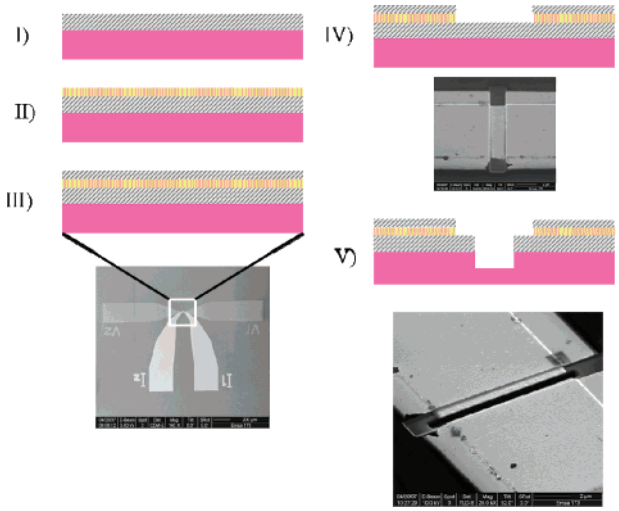

Figure 2. Manufacturing process of 3-D chips: (I) first layer of Pt structures built by photolithography, physical vapor deposition and lift off; (II + III) layer of SiN evaporated on the first layer of Pt isolates both Pt layers; (IV + V) definition of electrodes by cutting out trenches by FIB milling in two steps; (V) final 3-D design and a SEM picture of 3-D chip.

electrode shape was realized in two FIB milling steps: (1) Separation of the electrodes in the upper layer of Pt by milling a trench. (2) Separation of the lower Pt electrodes by cutting a trench into the lower cleared Pt layer.

Within the first step we sectioned a rectangular trench of 1500 nm width and approximately 15 μm height in the middle of the layer-overlapping area (Figure 2(IV)). In doing so, we uncovered the lower Pt layer completely within the area of the rectangular trench by removing the Pt of the top layer and the SiN beneath. A small ion current of 100 pA was used to avoid a too fast milling rate, which could result in damaging parts of the lower Pt layer.

Next, within the second milling step, we separated the lower, cleared Pt electrodes from each other. Again, we used a rectangular milling pattern with a width of 500 nm and a height of approximately 15 μm (Figure 2(V)). Because we are interested in suspended CNTs, a deep trench between the opposing lower electrodes was cut by an increased ion current of 300 pA into the SiN layer beneath the lower Pt layer. These 3-D chips (Figure 2(V)) have been electrically contacted to a ceramic package by wire-bonding and are ready for dielectrophoretic integration of CNTs.

For the deposition of MWCNTs by DEP, the chip was wired specifically for this purpose. To this end, on each side of the central gap, only the outermost electrode was connected to the electrical circuit. We placed a droplet of a CNT suspension on the wired chip and applied an electric alternating voltage ($f = 5$ MHz) to the wired electrodes. The CNT suspension was composed of ethanol, containing diluted CNTs. For the preparation of the CNT suspension, commercially available MWCNTs, supported by NanoLab and Helix, and pure ethanol were used. In some cases the CNT suspension was enriched with sodium dodecyl sulfate (SDS). A more detailed description of the suspension preparation process is provided elsewhere.[15]

Table 1. Comparison of the DEP Deposition Yield between Au and Pt as Electrode Materials for Test Chips

material	CNT diameter (nm)	no. of positions	yield (%)
Au	30	93	39
Pt	30	267	11

The DEP study has been carried out with three types of MEMS chips. "Test chips", which are easy and inexpensive to manufacture, have been used to estimate the influence of the electric field magnitude, the influence of the electrode material, and the influence of CNT concentration in the ethanol suspension on the yield of successful CNT deposition. These test chips contain two elliptic electrodes, contrary to the previously described 2-D and 3-D chips, separated by a gap.[16]

In the case where a CNT had been successfully deposited onto a 3D-chip, platinum was soldered by electron beam deposition onto each of the four contact points of the CNT and the platinum electrodes. The soldering was carried out in the same FIB as for the chip milling and yielded the reduction of the contact resistance between the deposited CNT and the Pt electrodes beneath.

The gained experience from the DEP experiments with test chips, offering two-point contacting, will be discussed in the following section.

To the best of our knowledge, the electrode material has not been investigated as a DEP parameter influencing the deposition yield of CNTs. In terms of contact resistance, Krupke et al.[17] reported that they observed a difference for carboxyl functionalized single-walled CNTs (SWCNTs) attached to either gold (Au) or silver (Ag). They found that functionalized SWCNTs exhibit lower contact resistances attached to a Ag electrode than to a Au electrode. They speculated that due to the functional carboxyl groups on the SWCNT surface, the CNTs have a higher affinity to Ag surfaces, resulting in better electrical contact. Furthermore, they observed that a higher number of SWCNT bundles have been attracted onto each pair of Au electrodes than onto Ag electrodes.

Our investigation aimed at clarifying the behavior of nonfunctionalized MWCNTs during their deposition by DEP over electrodes of different materials in terms of successful deposition yield. We compared Pt electrodes on test chips with Au electrodes on test chips because these materials are commonly used as electrode materials. Our results reflecting two series of DEP experiments with test chips are shown in Table 1. We define the deposition yield for the test chip design as the ratio of electrode positions where at least one CNT bridged the electrode gap to the total amount of electrode positions tested. We found that the deposition yield is significantly higher over Au electrodes (ca. 40%) than over Pt electrodes (ca. 11%). The result for Pt electrodes is an average of three different suspension concentrations of diluted MWCNTs. The dependence of the suspension concentration on the deposition yield will be discussed later. It is important to emphasize in advance that the yield over

Pt electrodes never reached the yield over Au electrodes for any level of suspension concentration.

Krupke et al. observed more attracted SWCNTs per pair of Au electrodes than for Ag electrodes using functionalized SWCNTs. Our findings support this observation based on nonfunctionalized MWCNTs. Additionally, our findings show that the deposition yield for a series of electrode pairs is drastically improved when using Au electrodes.

Despite the better deposition yield using Au, we selected Pt as material for our electrodes because Au electrodes were more often damaged during the DEP experiments than Pt electrodes. We suspect that Pt is less sensitive to the voltage applied to the electrodes during the DEP than Au. Another reason for us to build Pt electrodes is explained by the FIB postprocessing. Gold appeared to have the disadvantage that, after milling, the electrode's edges are rough and material of the designated electrodes was removed. The Pt electrodes did not show any significant loss of electrode material nor rough edges.

The electric field that is applied during the DEP and the resulting DEP force are directly correlated to each other. A theoretical correlation between the applied voltage and the deposition yield does not exist. In the past years research groups addressed this lack of knowledge and determined optimum conditions for their specific environment.[17,18] Systematic studies by Chen et al.[19] identified the applied electric field as a key factor for successful CNT deposition by DEP. Furthermore, Chung et al.[2,20] presented a study in which they stated an empirical optimum electric field of 0.544 $V_{rms}/\mu m$ for the deposition of individual MWCNTs.

Herein we investigated the deposition of individual MWCNTs with a diameter of 10 nm. During the DEP experiments with test chips we applied a voltage composed of an ac part with a dc offset. In several experimental series the electric field strength was varied. The electric field was changed either by varying the magnitude of the total voltage ($V = V_{rms} + V_{dc}$) or by varying the electrode gap distance between the two opposing electrodes.

The results of our DEP study with test chips are displayed in Figure 3. The applied total voltage is plotted against the electrode gap distances. The straight lines within the diagram classify sectors of electric field strength. We divided the spectrum of electric fields applied during the DEP experiments into nine sectors, E1−E9, with electric field strengths from 0.027 V/μm (E1) to >2.4 V/μm (E9). In each sector we tested 96 pairs of electrodes. Furthermore, Figure 3 relates each sector of electric field strength with a corresponding deposition yield. According to our results, the deposition yield increases with increasing electric field strength. The observed deposition yield varied between 0% for very small electric field strength and 16% for moderate electric field strength. A low deposition yield, which is not 0%, could be observed for electric field strengths higher than 1.6 V/μm. Beyond this threshold value the deposition yield decreases again, which can be explained by an increasing probability to attract CNT bundles blocking the gap. Under the given conditions we found that the optimal electric field strength is located between ~0.8 and ~1.6 V/μm, i.e., sectors E6 and E7. The optimum electric field strength described by Chung is located in sector E5, 0.535−0.816 V/μm. Contrary to Chung[20,2] we observed the third best yield at E5 with a significantly lower deposition yield than E6 and E7. Because we used test chips with Pt electrodes instead of Au electrodes, as Chung did, we observed a general lower deposition yield than Chung.[2]

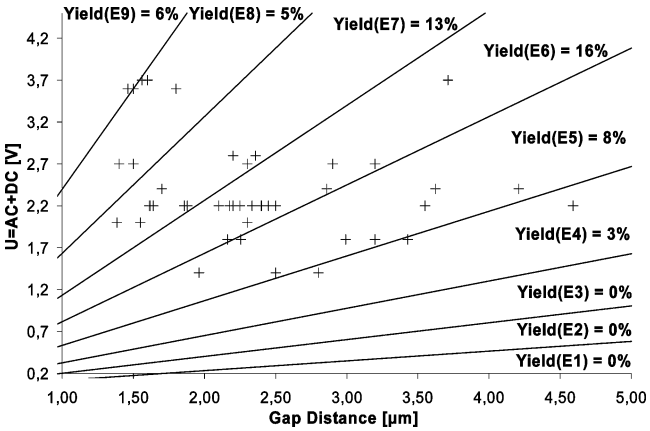

Figure 3. DEP deposition result for test chips with 10 nm diameter MWCNTs plotted for the applied voltage over the electrode gap distance between the electrodes. A "+" sign marks a successfully deposited CNT. The applied electric fields are categorized in sectors E1−E9, which are indicated by straight lines in the diagram. The deposition yield for each sector is given as "yield" in the diagram.

Table 2. Yield Dependence on the Concentration of Diluted CNTs in Ethanol Suspension for Test Chips

concn (μg/mL)	CNT diameter (nm)	no. of positions	Yield
0.033	30	72	4
0.11	30	89	11
0.165	30	106	16

For the deposition of CNTs onto four-point electrode structures a deep experimental understanding of DEP is necessary. Besides the electrode's material and the electric field strength, the concentration of CNTs diluted in the suspension is of major importance for the deposition yield. Previous studies did not investigate systematically this influence. Herein, we report that the suspension concentration influences the success of CNT deposition. Three different suspension concentrations have been investigated, 0.033, 0.11, and 0.165 μg/mL (μg of MWCNT/mL of ethanol), with test chips, and benchmarked according to the deposition yield of each. Table 2 presents the results of this study. We found that the deposition yield improves linearly with increasing concentration. For the low concentration suspension of 0.033 μg/mL, a yield of 4% has been observed. If the concentration is increased to 0.11 μg/mL, an improved yield of 11% could be achieved. Finally, the maximum yield of 16% was found for the highest concentrated suspension (0.165 μg/mL). The results are explained by the probability of finding a CNT in the vicinity of the desired deposition position. Because the attractive force resulting from the electric field between the electrode gap is limited in range, at least one CNT must be present within that range. The

Table 3. Comparison of the CNT Deposition Yield over Different Four-Point Electrode Designs

design	no. of positions	yield (%)
2-D	88	3.5
3-D	59	24
3-D[a]	40	40

[a] With SDS modified ethanol-CNT suspension.

probability of finding a CNT within the DEP force range increases with the CNT concentration of the suspension.

Reviewing the literature that also reports suspension concentrations over two-point electrode structures,[21−24] we should prove that the deposition yield for individual CNTs will not further increase beyond a certain threshold level of suspension concentration. Beyond that certain threshold value of concentration level, the density of CNTs per volume suspension is so high that it becomes impossible to attract an individual CNT. Hence, the yield for the deposition of individual unbundled CNTs would decrease. This finding is supported by Subramanian et al.[24] who tested suspension concentrations of 2 and 0.5 μg/mL. They were able to deposit individual CNTs using 0.5 μg/mL suspensions whereas they deposited mainly CNT bundles but no individual CNTs using the higher concentrated suspension. Reported concentrations of 0.01−0.05 mg/mL were used to manufacture sensors based on CNT bundles,[21−23] which additionally confirms our theory.

Our DEP experiments with test chips provided a deeper knowledge of the most important parameters influencing the successful deposition of individual MWCNTs over a two-point electrode gap. This knowledge was applied to the deposition of suspended, individual MWCNTs over four-point electrode structures. The four-point MWCNT deposition was investigated for both introduced 2-D (Figure 1) and 3-D (Figure 2) designs. Table 3 summarizes the results of the deposition experiments. It becomes clear that 3-D structures have a superior deposition yield of 24% that is more than 6 times higher than that for the tested 2-D structures. For four-point electrode structures, we define the deposition yield as the ratio of electrode positions where a suspended, individual CNT crossed all four electrodes to the total number of tested electrode positions. The key to the superior deposition yield of 3-D chips compared to 2-D chips is the gap design. For the conventional 2-D design approach, four electrodes are placed in one plane. This results in three gaps with three separated electric fields in between. As a consequence we often observed during the DEP with 2-D chips that CNTs have been deposited over only one or two of the three gaps. Contrary to the 2-D chips, the 3-D design offers four electrodes but only one gap, which has to be crossed by a CNT. In the literature only a few reports exist on the deposition of suspended, individual four-point contacted CNTs and the yield of the deposition process. Lewenstein et al.[10] reported a yield of 20−55% for their method. However, unlike our definition of deposition yield, they also counted CNTs deposited over only the two innermost electrodes as a successful deposition. This renders a comparison of Lewenstein's[10] results with our results of real four-point contacted CNTs meaningless.

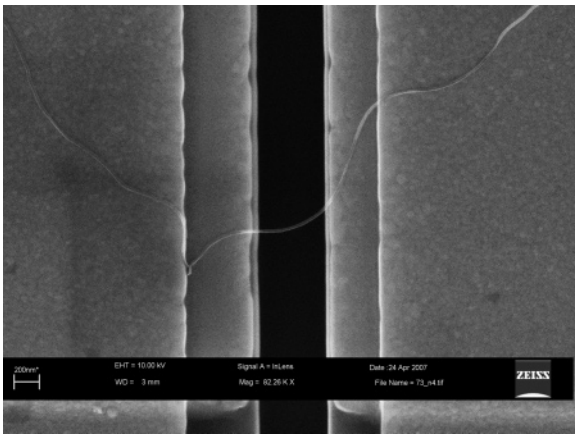

Figure 4. Example of a successfully deposited individual, suspended MWCNT with a diameter of 30 nm onto a 3-D chip.

Comparing the deposition yield of the four-point 2-D structures to that of two-point Pt electrodes results in a significantly lower deposition yield in the former case. This can be a result of a less optimal electric field distribution due to the presence of additional electrodes with higher probability for a failed deposition. To this end, CNTs often crossed less than four electrodes, and this was not counted as successful deposition.

After we evaluated the 3-D design as superior, we investigated the possibility of further enhancing the deposition yield by modifying the ethanol suspension. In the experiments heretofore, we experienced that bundles of CNTs often blocked the electrode gap and prohibited a successful deposition of suspended, individual MWCNTs. The use of SDS was aimed to reduce the amount of bundled CNTs in the suspension, which thereby reduces the probability of attracting a bundle to the electrode gap and thus increases the deposition yield. We tested an ethanol−CNT suspension enriched with 1 mass % of SDS. Table 3 shows that the effect of reduced bundle attraction could be realized. A significantly higher yield of 40% compared to 24% with pure ethanol suspensions was observed. This high yield enables the reliable building of devices based on suspended, individual four-point contacted MWCNTs. Figure 4 shows an example of a successful deposition onto a 3-D chip. The individual MWCNT with a diameter of 30 nm crosses the inner gap of 0.5 μm suspended and connects each of the four electrodes electrically.

A drawback of MWCNTs deposited with the SDS enriched suspension was that they broke more often during the sensor postprocessing due to electric discharge. We speculate that a monolayer of SDS molecules attached to a CNT surface alters the current transport capabilities of CNTs.

In conclusion, we have reported a systematic study of the most important parameters for the successful deposition of suspended, individual MWCNTs onto MEMS by DEP. In a further step we made use of the acquired knowledge of MWCNT deposition by DEP, developing a method to deposit MWCNTs over four-point electrode structures. The achieved

four-point deposition yield for 3-D structures aids the realization of CNT devices.

Acknowledgment. The financial support of the ETH Forschungskommission is kindly acknowledged.

References

(1) Zhang, Y. G.; Chang, A. L.; Cao, J.; Wang, Q.; Kim, W.; Li, Y. M.; Morris, N.; Yenilmez, E.; Kong, J.; Dai, H. *J. Appl. Phys. Lett.* **2001**, *79*, (19), 3155−3157.
(2) Chung, J. Y.; Lee, K. H.; Lee, J. H.; Ruoff, R. S. *Langmuir* **2004**, *20*, (8), 3011−3017.
(3) Pohl, H. A. *J. Appl. Phys.* **1951**, *22*, (7), 869−871.
(4) Kim, J. E.; Han, C. S. *Nanotechnology* **2005**, *16*, (10), 2245−2250.
(5) Dimaki, M.; Boggild, P. *Nanotechnology* **2004**, *15*, (8), 1095−1102.
(6) Martel, R.; Schmidt, T.; Shea, H. R.; Hertel, T.; Avouris, P. *Appl. Phys. Lett.* **1998**, *73*, (17), 2447−2449.
(7) Dockendorf, C. P. R.; Steinlin, M.; Poulikakos, D.; Choi, T. Y. *Appl. Phys. Lett.* **2007**, *90*, (19).
(8) Li, J.; Lu, Y. J.; Ye, Q.; Delzeit, L.; Meyyappan, M. *Electrochem. Solid State Lett.* **2005**, *8*, (11), H100−H102.
(9) Dohn, S.; Molhave, K.; Boggild, P. *Sensor Lett.* **2005**, *3*, (4), 300−303.
(10) Lewenstein, J. C.; Burgin, T. P.; Ribayrol, A.; Nagahara, L. A.; Tsui, R. K. *Nano Lett.* **2002**, *2*, (5), 443−446.
(11) Klinke, C.; Hannon, J. B.; Afzali, A.; Avouris, P. *Nano Lett.* **2006**, *6*, (5), 906−910.
(12) Ebbesen, T. W.; Lezec, H. J.; Hiura, H.; Bennett, J. W.; Ghaemi, H. F.; Thio, T. *Nature* **1996**, *382*, (6586), 54−56.
(13) Schoenenberger, C.; Bachtold, A.; Strunk, C.; Salvetat, J. P.; Forro, L. *Appl. Phys. A: Mater. Sci. Processing* **1999**, *69*, (3), 283−295.
(14) Gao, B.; Chen, Y. F.; Fuhrer, M. S.; Glattli, D. C.; Bachtold, A. *Phys. Rev. Lett.* **2005**, *95*, (19).
(15) Choi, T. Y.; Poulikakos, D.; Tharian, J.; Sennhauser, U. *Nano Lett.* **2006**, *6*, (8), 1589−1593.
(16) Choi, T. Y.; Poulikakos, D.; Tharian, J.; Sennhauser, U. *Appl. Phys. Lett.* **2005**, *87*, (1).
(17) Krupke, R.; Hennrich, F.; Weber, H. B.; Beckmann, D.; Hampe, O.; Malik, S.; Kappes, M. M.; Löhneysen, H. V. *Appl. Phys. A: Mater. Sci. Processing* **2003**, *76*, (3), 397−400.
(18) Lu, S.; Chung, L.; Ruoff, R. S. *Nanotechnology* **2005**, *16*, 1765−1770
(19) Chen, X. Q.; Saito, T.; Yamada, H.; Matsushige, K. *Appl. Phys. Lett.* **2001**, *78*, (23), 3714−3716.
(20) Chung, J.; Lee, J. *Sens. Actuators A: Physical.* **2003**, *104*, (3), 229−235.
(21) Fung, C.; Wong, V. T. S.; Chan, R. H. M.; Li, W. J. *IEEE Trans. Nanotechnol.* **2004**, *3*, (3), 395−403.
(22) Dimaki, M.; Boggild, P. *Phys. Status Solidi A: Appl. Mater. Sci.* **2006**, *203*, (6), 1088−1093.
(23) Chan, R. H. M.; Fung, C. K. M.; Li, W. J. *Nanotechnology* **2004**, *15*, (10), 672−S677.
(24) Subramanian, A.; Vikramaditya, B.; Nelson, B. J.; Bell, D.; Lixin, D. *Advanced Robotics, ICAR '05 Proc.* **2005**, 208−215.

NL071853T